RSC Applied Polymers

ROYAL SOCIETY OF CHEMISTRY

COMMUNICATION

View Article Online
View Journal | View Issue

Check for updates

Cite this: *RSC Appl. Polym.*, 2024, **2**, 26

Received 27th September 2023,
Accepted 26th November 2023

DOI: 10.1039/d3lp00178d

rsc.li/rscapplpolym

Strengthening ethylene-methacrylic acid ionomers with single-boron-based molecules as cross-linkers in dynamic networking†

Peng Wen,[a] Yang Zeng,[a] Lu Zhang,[a] Tao Wang,[b] Jeffrey M. Cogen,[c] Colin Li Pi Shan,[c] Yixuan Liu[a] and Mao Chen *[a]

We report the employment of single-boron compounds as readily available cross-linkers for strengthening ethylene-methacrylic acid ionomers. The novel cross-linking strategy effectively strengthened the ionomers with enhanced mechanical and rheological properties, affording excellent (re)processability without changing the transparent appearance.

Semi-crystalline ionomers composed of polyethylene-*co*-methacrylic acid partially neutralized by metal cations such as sodium, zinc or others, known as SURLYN™, are important industrial materials.[1–5] Such ionomers are characterized by the presence of strong electrostatic interactions between metal cations and carboxylates in cluster domains, as well as crystalline domains from polyethylene segments (Fig. 1).[6–8] The combination of two physical interactions into one system dramatically enhances the mechanical properties of the ionomer, including high tensile strength, good stiffness, and outstanding resistance to abrasion/puncture, some of which are even better than those of crystalline polyethylene and its copolymers with carboxylic acid.[9]

In recent years, polymers with dynamic networks have received great research interest.[10–16] The incorporation of dynamic covalent/non-covalent interactions into polymer matrices has furnished promising solutions to improve physical properties without losing the ability to be (re)processed, allowing cross-linked polymers to be reconfigured like thermoplastics.[10–13] A variety of chemical and physical interactions have been shown to fulfill demands in various chemical structures.[10–15] Among many elegant approaches, polymer networks derived from boron chemistry have displayed rapid and reversible thermodynamic responses,[17,18] enabling covalent adaptable networks for polymers including polyethylene,[19] polystyrene,[20] poly(methyl methacrylate),[20,21] poly(dimethylsiloxane)[22] and others.[23–31] For example, Sumerlin,[24,25] Guan,[23] Leibler[19,20] and Guo[27] demonstrated the employment of boronic esters as reconfigurable dynamic bonds to yield high-performance materials. You[22] and Guan[26] disclosed malleable thermosets based on boroxine networks. Our group reported strategies of dynamic covalent macro-cross-linkers[32] and polymer network additives[33] based on boronic esters to strengthen commodity thermoplastics. Previous methods with boron-based multi-arm cross-linkers have successfully expanded opportunities toward reconfigurable thermosets.

Due to the strong Lewis acidity, boron compounds (*e.g.*, boronic acids, boronic esters, *etc.*) have been applied in studies ranging from biomolecule adsorption,[34] organic transformation[35–37] and so on,[38] where the sp^2 hybrid boron centre transforms into a sp^3 hybrid centre coordinated with one or more carboxylate groups. Those studies are different from the ones utilizing boronic esters or boroxines in dynamic covalent networks, and represent a weaker interaction between boron atoms and nucleophiles. Inspired by these results, we hypothesized that organic molecules with single boron atoms could be adopted as novel cross-linkers for carboxylates in ionomers. In this work, we report the investigations of employing single-boron-based compounds as readily available additives for ionomers, demonstrating that boron compounds of higher Lewis acidities exhibit stronger interactions with carboxylate groups. Studies on the mechanical and rheological properties indicate that rational selection of boron compounds could enhance Young's modulus, yield strength, creep resistance, and storage/loss modulus of an ionomer without compromising the advantages of (re)processability, transparent appearance, *etc.*

At the beginning of this work, in order to investigate the Lewis acidity of boron compounds, which is used as the basic parameter to evaluate the strength of their interactions with electron-donating groups (carboxylates) in ionomers, we exam-

[a]*Department of Macromolecular Science, State Key Laboratory of Molecular Engineering of Polymers, Fudan University, Shanghai 200433, China. E-mail: chenmao@fudan.edu.cn*
[b]*Dow Chemical China Holding Company, Shanghai 201203, P.R. China*
[c]*Dow Chemical Company, USA*

† Electronic supplementary information (ESI) available. See DOI: https://doi.org/10.1039/d3lp00178d

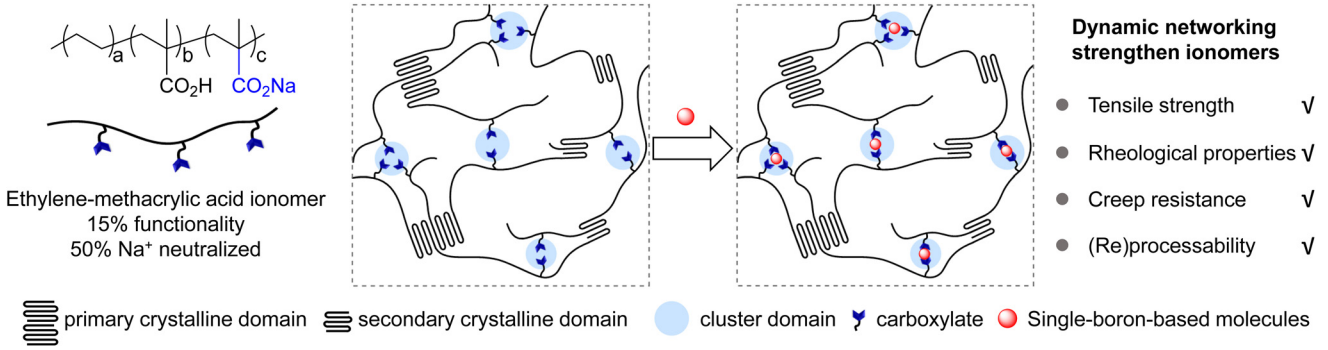

Fig. 1 Structure and physical interactions of the unmodified and modified ionomers.

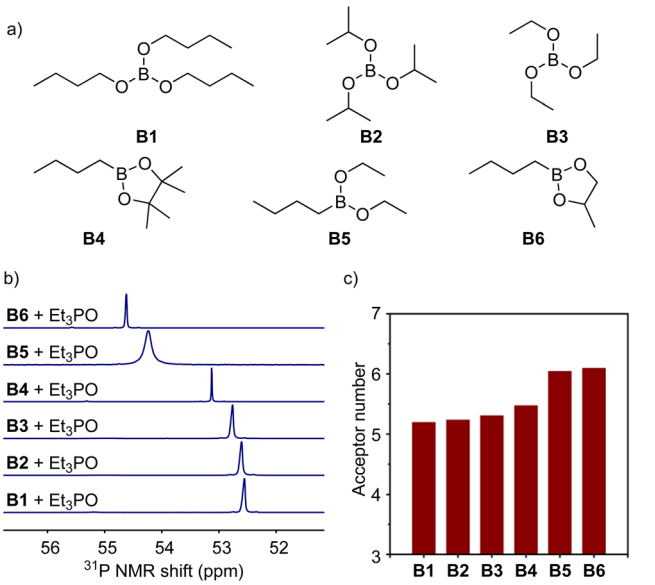

Fig. 2 (a) Chemical structures of boron compounds studied in this work (**B1** to **B6**). (b) ^{31}P NMR results of $Et_3P{=}O$ in the presence of boron compounds. (c) Acceptor numbers of boron compounds determined by the Gutmann–Beckett method.

ined the acceptor numbers of a variety of boron compounds (Fig. 2a) including tri-*n*-butyl borate (**B1**), triisopropyl borate (**B2**), triethyl borate (**B3**), *n*-butylboronic acid pinacol ester (**B4**), *n*-butylboronic acid diethyl ester (**B5**), and *n*-butyl boronic acid cyclic propylene ester (**B6**) by the Gutmann–Beckett method to quantify the Lewis acidity.[39,40] As analysed by phosphine nuclear magnetic resonance (^{31}P NMR), triethylphosphine oxide ($Et_3P{=}O$) gave increasing values of ^{31}P chemical shifts after being coordinated with molecules from **B1** to **B6**, resulting in increasing acceptor numbers from 16.6 to 21.2 (Fig. 2b and c). The experimental results suggest that the six boronic esters afford different Lewis acidities, and alkyl boronic esters (**B4** to **B6**) possess higher Lewis acidities than trialkyl borates (**B1** to **B3**). Because of the poor compatibility with boronic acid (*e.g.*, aryl boronic acid), mixing with boronic acid caused an apparent appearance change in the ionomer, leading to opaque samples. Moreover, many commercially available trialkyl boranes and dialkyl alkoxyl boranes are unstable under air atmosphere. Such compounds were not explored in this study.

According to the acceptor number, the Lewis acidities of boron compounds increased from **B1** to **B6**. To probe the interaction between the carboxylate group and boron compounds, we conducted density functional theory (DFT) calculations. As summarized in Fig. 3a, while the binding energies between boron compounds and sodium acetate (NaOAc) all give negative values in a range from −0.19 to −0.35 eV, indicating exothermic transformations to form the corresponding coordinated species, the energies obtained with **B5** and **B6** are higher than those with the other four boron compounds, which are consistent with their higher Lewis acidities. When two NaOAc units interact with one boron molecule, the adoption of **B5** furnishes a bonding energy of −0.56 eV, implying the possibility of employing **B5** as a cross-linker to interact with multiple carboxylate pendants in the ionomer. Different from coordination with one acetate group, the interaction with two NaOAc units is more likely to form an ionic cluster based on the B–O distances by calculations (Fig. 3b).

In order to investigate the effect of boron compounds on the crystal domain of the ethylene-methacrylic acid ionomer, differential scanning calorimetry (DSC) and wide-angle X-ray scattering (WAXS) tests were conducted. Firstly, the unmodi-

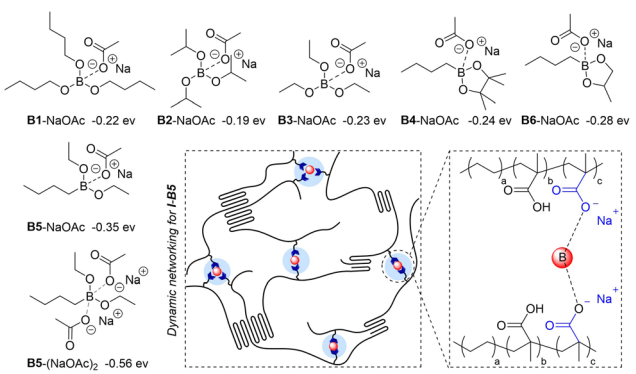

Fig. 3 DFT calculations of binding energies between boron compounds and sodium acetate (NaOAc) and illustration of dynamic networking of **I-B5**.

fied ionomer and modified ionomers from **I-B1** to **I-B6** were characterized by differential scanning calorimetry (DSC) at a scanning rate of 10 °C min^{-1} to analyse melting temperatures and enthalpy changes. As shown in Fig. 4a (Fig. S10–S13†), all samples clearly exhibit two melting points (T_{m1} and T_{m2}), which correspond to primary and secondary crystallinities,[4,41] respectively. While **I**, **I-B1**, **I-B2** and **I-B3** exhibit T_{m1} (93.7–93.9 °C) and T_{m2} (50.2–50.6 °C) in narrow ranges, samples from **I-B4** to **I-B6** exhibit lower melting points of T_{m1} = 88.8–90.6 °C and larger deviations of T_{m2} (46.1–52.3 °C). In comparison with **I**, **I-B5** shows decreased endotherms (ΔH_{m1} = 37.05 *vs.* 40.56 J g^{-1} in Fig. 4b and ΔH_{m2} = 6.15 *vs.* 8.23 J g^{-1} in Fig. 4c), attributed to the declined degrees of crystallinities in primary and secondary domains (12.6% *vs.* 13.8% for primary crystallinity and 2.1% *vs.* 2.8% for secondary crystallinity). Decreased endotherms for secondary crystallinities are also observed in **I-B4** and **I-B6**.

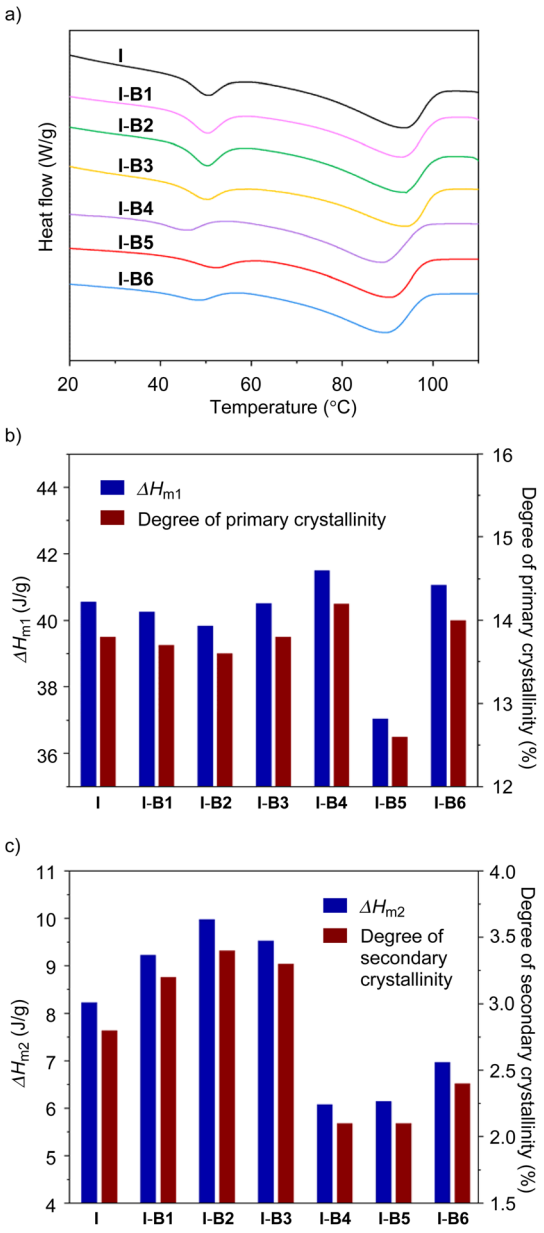

Fig. 4 (a) DSC curves of the ionomer and samples from **I-B1** to **I-B6** at a scanning rate of 10 °C min^{-1}. (b) Heat of fusion (ΔH_{m1}) and degree of primary crystallinity (%) and (c) heat of fusion (ΔH_{m2}) and degree of secondary crystallinity (%) of the ionomer and **I-B1** to **I-B6**.

The variations in melting points and endotherms are caused by the impact of boron compounds (**B4** to **B6**) on crystalline domains. We hypothesize that because **B4** to **B6** display higher Lewis acidities than **B1** to **B3**, the addition of such molecules improves interactions in cluster areas, and further affects the formation of crystalline domains. Since **B4** exhibits much higher steric hindrance and a lower bonding ability with carboxylate, cyclic compounds of **B4** and **B6** are less favourable to interact with multiple carboxylates as supported by DFT calculations (Fig. S5 and S6†), and the use of **B4** and **B6** only decreases the secondary crystalline domains. In contrast, although the addition of **B5** decreased both crystalline domains, this single-boron-based compound could effectively interact with multiple carboxylates and act as a cross-linker in the ionomer matrix. Overall, according to the DSC results, **I-B5** exhibited the lowest total crystallinity among all the modified ionomers, which is also consistent with the WAXS results (Fig. S14†), which may result in the improvement of the mechanical and rheological properties.

To demonstrate the ease of processing, we employed a mechanical mixing process to mix boron compounds and an ionomer at 160 °C. An ionomer having 15% methacrylic acid as a co-monomer and 50% of the acid group neutralized by Na^+ was selected as the control (sample **I**). The melt index (MI) is 5 dg min^{-1}, according to a standard method of ASTM D1238-23 (at 190 °C and 2.16 kg).[42] The boron compound (2.5 wt%) and the ionomer (**I**) were mechanically stirred in an internal mixer in the melt state. After mixing, the materials were processed by hot pressing, and cut into a dumbbell shape for tensile test experiments at room temperature to evaluate the mechanical properties. As shown in Fig. 5a, the ionomer (**I**) and its composites (**I-B1** to **I-B6**) exhibit tensile strengths in a range of about 20–36 MPa. Although **I-B5** and **I-B6** resulted in slightly lower tensile strengths, their Young's moduli and yield strengths are higher than those of the unmodified ionomer (Fig. 5b and c), which may be caused by the interaction with ionomers using the boron compound as the cross-linker. Among all the examined compounds, **B5** has the highest binding energy with the carboxylate group as supported by simulations, which suggested that the addition of **B5** could form a more stable network with ionomers, thus effectively improving the strength and stiffness of ionomers. For example, **I-B5** exhibits a Young's modulus of 251 MPa and a yield strength of 22 MPa, while the two values measured for the ionomer control sample are 114 MPa and 15 MPa, respectively, demonstrating an improved mechanical strength. The yield ratio determined by yield strength and tensile strength is employed to illustrate the strain hardening. As shown in Fig. 5d, samples from **I-B4** to **I-B6** exhibit clearly enhanced yield point ratios as compared to the ionomer, where improve-

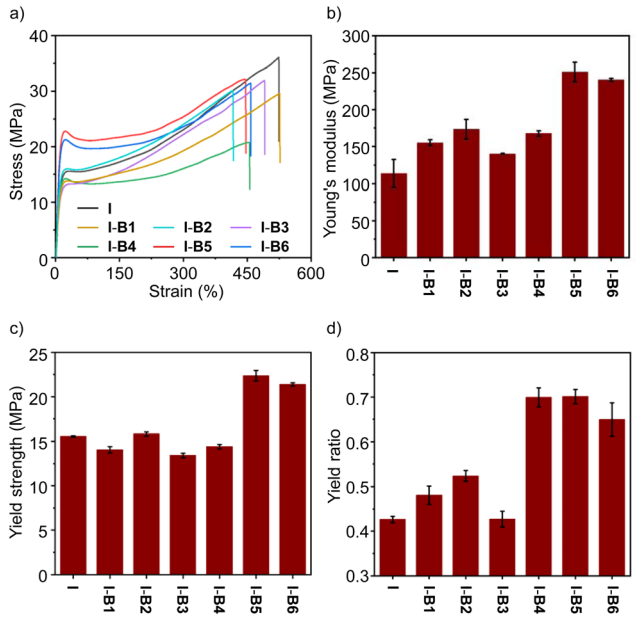

Fig. 5 (a) Stress–strain curves of the ionomer (I) and samples from **I-B1** to **I-B6** conducted at 25 °C. (b) Young's modulus, (c) yield strength and (d) yield ratio [(yield strength)/(tensile strength)] of the ionomer and samples from **I-B1** to **I-B6**.

ments in **I-B5** and **I-B6** are caused by the higher yield strengths, and the increase in **I-B4** is attributed to the clearly declined tensile strength. The yield ratio of **I-B5** is about 1.7 times that of the unmodified ionomer. In addition, the stability of **I-B5** in water was investigated. As shown in Fig. S15,† the tensile properties of **I-B5** did not undergo a dramatical change before and after being soaked in water for 3–10 days, suggesting the good water stability of the crosslinked material. **I-B5** exhibits good solvent resistance as supported by the low swelling ratios in a variety of organic solvents (Table S3†).

The physical properties at elevated temperatures could influence the application and processing technique of ionomers. In order to investigate the mechanical properties and creep resistance of modified ionomers at high temperature, the tensile tests and creep tests were conducted at 70 °C and 75 °C, respectively. When the tensile tests were conducted at 70 °C, samples from **I-B2** to **I-B6** displayed higher tensile strengths (12.1–16.5 *vs.* 9.7 MPa, Fig. 6a) and Young's moduli (20.2–22.8 *vs.* 14.1 MPa, Fig. 6b) as compared to the unmodified ionomer, with the yield strength increasing from 3.2 MPa to about 4.2 MPa. Creep resistance experiments were performed with dumbbell-shaped samples by loading extra weight at 75 °C for 40 min (Fig. 6c). As illustrated in Fig. 6d, **I-B3**, **I-B5** and **I-B6** exhibit clearly lower deformation than the ionomer control, whereas **I-B5** provides the best resistance against deformation, confirming that creep resistance is successfully improved by adding boron compounds. The Lewis acidic boron cross-linkers could broaden the application scope of ionomers by improving their mechanical strength and creep resistance at high temperatures.

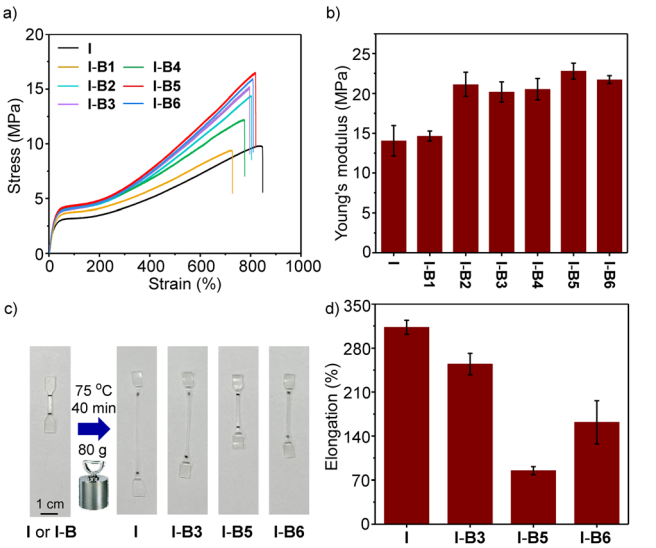

Fig. 6 (a) Stress–strain curves and (b) Young's modulus of the ionomer (I) and samples from **I-B1** to **I-B6** measured at 70 °C. (c) Optical images and (d) results of the elongation experiments of the ionomer, **I-B3**, **I-B5** and **I-B6** conducted at 75 °C.

The good reprocessability of ionomers is valuable toward sustainable polymer materials. We investigated the (re)processability of modified ionomers (**I-B5**) and their mechanical properties. As shown in Fig. 7a, the fragmentized ionomers (**I-B5**) were reprocessed *via* the mechanical mixing process and cut into samples of dumbbell shape after hot pressing, and the modified ionomers still maintain high transparency after reprocessing. This process was recycled three times. By conducting the tensile tests of **I-B5** at each time, the stress–strain curves are obtained and are shown in Fig. 7b; after reprocessing 3 times, **I-B5** maintains the elongation at around 450%. The Young's modulus and yield strength are summarized in

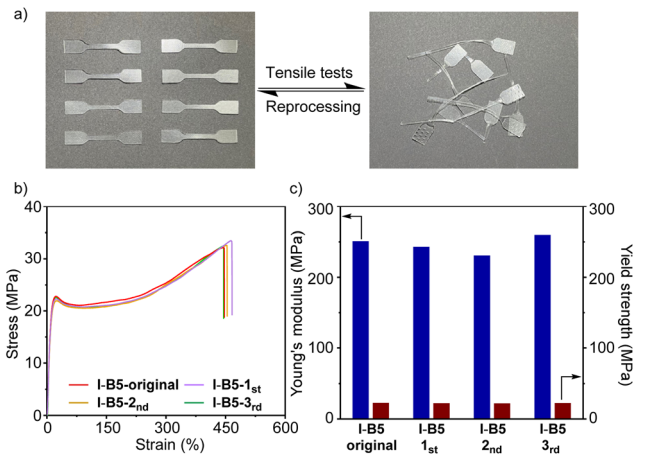

Fig. 7 (a) Image of the experiment for the investigation of the reprocessability of **I-B5**. (b) Stress–strain curves of original and recycled **I-B5**. (c) Young's modulus (blue column) and yield strength (brown column) results of original and recycled **I-B5**.

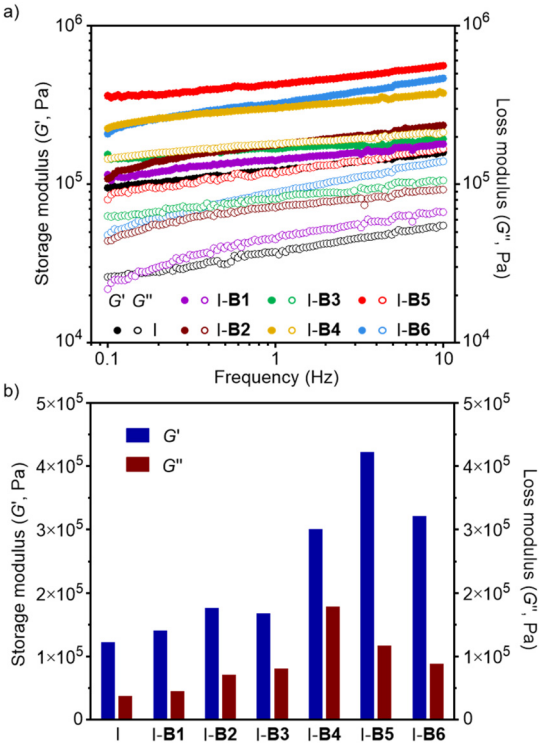

Fig. 8 (a) Storage (G') and loss moduli (G'') of the ionomer, **I-B1**, **B2**, **B3**, **B4**, **B5** and **B6** measured by frequency sweeps at 70 °C. (b) G' and G'' of the ionomer, **I-B1**, **B2**, **B3**, **B4**, **B5** and **B6** at 1 Hz.

Fig. 7c, **I-B5** maintained the original mechanical properties without exhibiting a dramatic change. These experiments suggest that **I-B5** with a dynamic network based on the interaction between ionomers and **B5** could be (re)processed *via* the mechanical mixing process without losing transparency and mechanical strength.

The storage (G') and loss moduli (G'') of ionomers **I-B1** to **I-B6** were measured by frequency sweeps in an oscillatory rheometer at 70 °C. As shown in Fig. 8a, all samples exhibit higher G' than G'' at different frequencies, showing agreement with their physically cross-linked structures with creep-resistant ability in the measured region. Moreover, the addition of boron compounds into the ionomer resulted in materials with improved G' and G'' as shown in Fig. 8b. For instance, **I-B5** exhibits storage and loss moduli about 3.5 and 3.1 times those of the ionomer (frequency = 1 Hz), respectively. On the basis of dynamic mechanical analysis (DMA), **I-B5** has the highest storage modulus (25 MPa) and the highest T_g (59.62 °C), suggesting the reduced chain mobility caused by the formation of the crosslinking network, which is beneficial for improving the mechanical performance of materials (Fig. S16†).

Conclusions

In this work, we demonstrate the employment of single-boron-based compounds as easily available additives for ethylene-methacrylic acid ionomers. The introduction of such boron compounds effectively improved the ionomer mechanical properties (*e.g.*, Young's modulus and yield strength), and enhanced the creep resistance and rheological properties at elevated temperatures. The interaction between boron and carboxylate provides polymers with excellent (re)processability without influencing the transparent appearance of the ionomer. Although the mixing with a boron compound (*e.g.*, **B5**) results in slightly decreased crystallinities, the single-boron-based molecule could act as a cross-linker for the ionomer. Given the broad applications of ionomers and increasing interest in improving polymers *via* dynamic interactions, this system provides an alternative path to strengthen ionomers using simple and low-cost additives, while maintaining their good (re)processability that could be easily handled using industry techniques.

Author contributions

P. Wen, Y. Zeng, and L. Zhang prepared the samples and conducted characterization; Y. Zeng, P. Wen and M. Chen conceived the idea; P. Wen conducted calculations; P. Wen, Y. Zeng, T. Wang and M. Chen analysed the results; Jeffrey M. Cogen, Colin Li Pi Shan and Yixuan Liu reviewed and edited the manuscript. T. Wang and M. Chen supervised the project and wrote the manuscript.

Conflicts of interest

There are no conflicts to declare.

Acknowledgements

We are thankful for the financial support from the Dow Chemical Company, Fudan University and State Key Laboratory of Molecular Engineering of Polymers.

References

1 S. Zhan, X. Wang and J. Sun, *Macromol. Rapid Commun.*, 2020, **41**, e2000097.
2 R. Dolog and R. A. Weiss, *Macromolecules*, 2013, **46**, 7845–7852.
3 E. Pregi, D. Kun, A. Wacha and B. Pukanszky, *Eur. Polym. J.*, 2021, **142**, 110110.
4 M. W. Spencer, M. D. Wetzel, C. Troeltzsch and D. R. Paul, *Polymer*, 2012, **53**, 569–580.
5 L. Lu and G. Li, *ACS Appl. Mater. Interfaces*, 2016, **8**, 14812–14823.
6 S. J. Kalista, J. R. Pflug and R. J. Varley, *Polym. Chem.*, 2013, **4**, 4910–4926.
7 Y. Gao, N. R. Choudhury and N. K. Dutta, *J. Appl. Polym. Sci.*, 2012, **124**, 2908–2918.

8 M. Aoyama, T. Koda, K. Miyata, T. Nishio and A. Nishioka, *Polym. Eng. Sci.*, 2015, **55**, 1843–1848.
9 C. Chen, *Nat. Rev. Chem.*, 2018, **2**, 6–14.
10 M. Guerre, C. Taplan, J. M. Winne and F. E. Du Prez, *Chem. Sci.*, 2020, **11**, 4855–4870.
11 B. R. Elling and W. R. Dichtel, *ACS Cent. Sci.*, 2020, **6**, 1488–1496.
12 Z. P. Zhang, M. Z. Rong and M. Q. Zhang, *Prog. Polym. Sci.*, 2018, **80**, 39–93.
13 Y. Gu, Y. Liu and M. Chen, *Chem*, 2021, **7**, 1990–1992.
14 X. Liu, Y. Li, X. Fang, Z. Zhang, S. Li and J. Sun, *ACS Mater. Lett.*, 2022, **4**, 554–571.
15 A. Rahman Md, C. Bowland, S. Ge, R. Acharya Shree, S. Kim, R. Cooper Valentino, X. C. Chen, S. Irle, P. Sokolov Alexei, A. Savara and T. Saito, *Sci. Adv.*, 2021, **7**, eabk2451.
16 C. Cui, L. An, Z. Zhang, M. Ji, K. Chen, Y. Yang, Q. Su, F. Wang, Y. Cheng and Y. Zhang, *Adv. Funct. Mater.*, 2022, **32**, 2203720.
17 A. P. Bapat, B. S. Sumerlin and A. Sutti, *Mater. Horiz.*, 2019, **7**, 694–714.
18 W. L. A. Brooks and B. S. Sumerlin, *Chem. Rev.*, 2016, **116**, 1375–1397.
19 R. G. Ricarte, F. Tournilhac, M. Cloître and L. Leibler, *Macromolecules*, 2020, **53**, 1852–1866.
20 M. Röttger, T. Domenech, R. van der Weegen, A. Breuillac, R. Nicolaÿ and L. Leibler, *Science*, 2017, **356**, 62–65.
21 S. Wu, H. Yang, W.-S. Xu and Q. Chen, *Macromolecules*, 2021, **54**, 6799–6809.
22 J.-C. Lai, J.-F. Mei, X.-Y. Jia, C.-H. Li, X.-Z. You and Z. Bao, *Adv. Mater.*, 2016, **28**, 8277–8282.
23 O. R. Cromwell, J. Chung and Z. Guan, *J. Am. Chem. Soc.*, 2015, **137**, 6492–6495.
24 J. J. Cash, T. Kubo, D. J. Dobbins and B. S. Sumerlin, *Polym. Chem.*, 2018, **9**, 2011–2020.
25 J. J. Cash, T. Kubo, A. P. Bapat and B. S. Sumerlin, *Macromolecules*, 2015, **48**, 2098–2106.
26 W. A. Ogden and Z. Guan, *J. Am. Chem. Soc.*, 2018, **140**, 6217–6220.
27 Y. Chen, Z. Tang, X. Zhang, Y. Liu, S. Wu and B. Guo, *ACS Appl. Mater. Interfaces*, 2018, **10**, 24224–24231.
28 B. Kang and J. A. Kalow, *ACS Macro Lett.*, 2022, **11**, 394–401.
29 Z.-H. Zhao, D.-P. Wang, J.-L. Zuo and C.-H. Li, *ACS Mater. Lett.*, 2021, **3**, 1328–1338.
30 S. Tajbakhsh, F. Hajiali and M. Marić, *ACS Appl. Polym. Mater.*, 2021, **3**, 3402–3415.
31 Z.-H. Zhao, P.-C. Zhao, Y. Zhao, J.-L. Zuo and C.-H. Li, *Adv. Funct. Mater.*, 2022, **32**, 2201959.
32 Z. Wang, Y. Gu, M. Ma and M. Chen, *Macromolecules*, 2020, **53**, 956–964.
33 Z. Wang, Y. Gu, M. Ma, Y. Liu and M. Chen, *Macromolecules*, 2021, **54**, 1760–1766.
34 R. J. Carvalho, J. Woo, M. R. Aires-Barros, S. M. Cramer and A. M. Azevedo, *Biotechnol. J.*, 2014, **9**, 1250–1258.
35 T. Hashimoto, A. O. Gálvez and K. Maruoka, *J. Am. Chem. Soc.*, 2013, **135**, 17667–17670.
36 K. Ishihara and Y. Lu, *Chem. Sci.*, 2016, **7**, 1276–1280.
37 S. Estopiñá-Durán, L. J. Donnelly, E. B. McLean, B. M. Hockin, A. M. Z. Slawin and J. E. Taylor, *Chem. – Eur. J.*, 2019, **25**, 3950–3956.
38 N. S. Hosmane and R. Eagling, *Handbook of Boron Science*, World Scientific, 2017.
39 U. Mayer, V. Gutmann and W. Gerger, *Monatsh. Chem.*, 1975, **106**, 1235–1257.
40 M. A. Beckett, G. C. Strickland, J. R. Holland and K. Sukumar Varma, *Polymer*, 1996, **37**, 4629–4631.
41 X. Wang, X. Li, C. Grimme, A. Olah, E. Baer and G. E. Wnek, *J. Appl. Polym. Sci.*, 2019, **136**, 48046.
42 ASTM D1238. 2023. Standard Test Method for Melt Flow Rates of Thermoplastics by Extrusion Plastometer.